

Supporting information

Broadband Blue Light Emissions of One-Dimensional Hybrid Cu(I) Halides with Ultrahigh Anti-Water Stability

Na Lin,^{ab} Yun-Xia Li,^a Yu Liu,^a Kai-Qi Sun,^a Hong-Yan Zhang,^a Xiao-Wu Lei,^{a*}

Zhi-Wei Chen^{a*}

^a Research institute of Optoelectronic Functional Materials, School of Chemistry, Chemical Engineering and Materials, Jining University, Qufu, Shandong, 273155, P. R. China

^b School of Chemistry and Chemical Engineering, Qufu Normal University, Qufu, Shandong, 273165, P. R. China

Corresponding Authors: Zhi-Wei Chen, Xiao-Wu Lei

E-mail: zw_chen@jnxy.edu.cn; xwlei_jnu@163.com

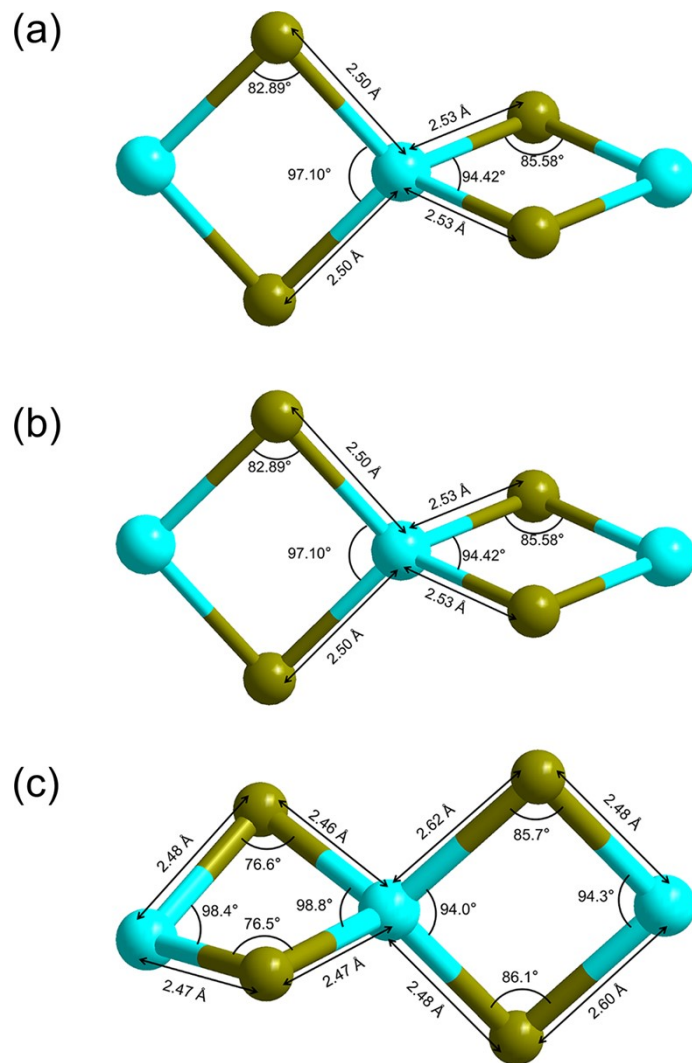


Fig. S1 The configurations of 1D $[\text{Cu}_2\text{Br}_4]^{2-}$ chain of (a) $[(\text{Me})_4\text{-Pipz}]\text{Cu}_2\text{Br}_4$, (b) $[\text{BuDA}]\text{Cu}_2\text{Br}_4$ and (c) $[\text{TMEDA}]\text{Cu}_2\text{Br}_4$.

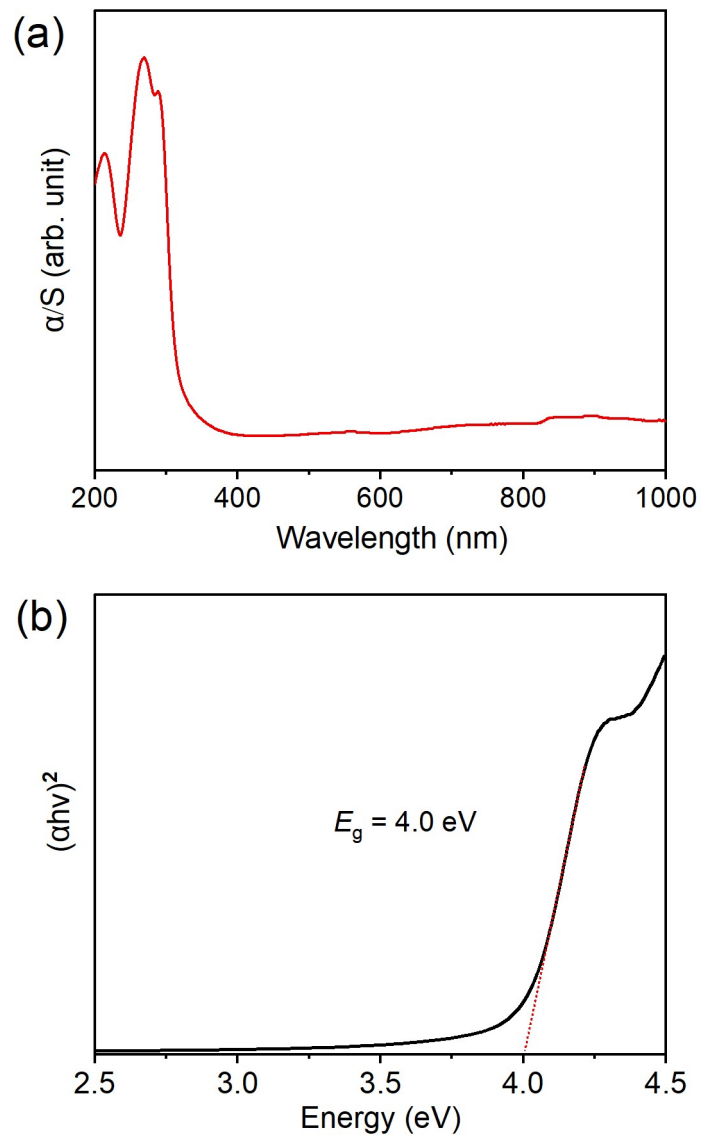


Fig. S2 The solid state UV-vis adsorption spectrum (a) and Tauc plot for band gap (b) of [(Me)₄-Pipz]Cu₂Br₄.

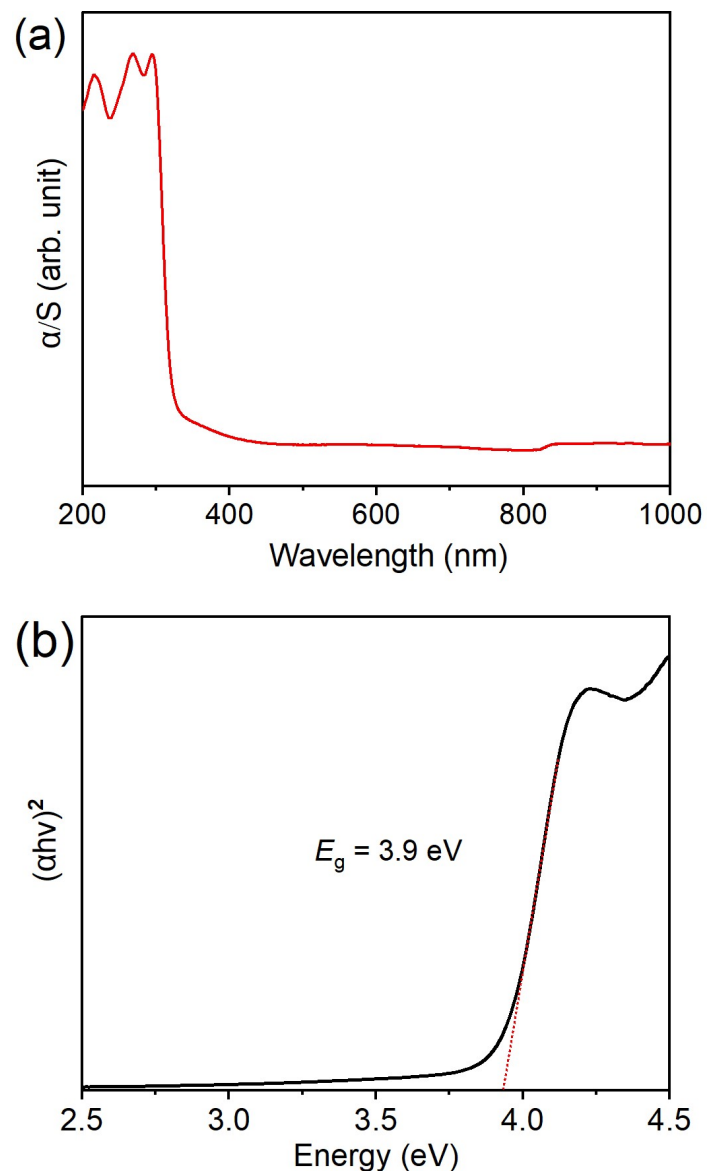


Fig. S3 The solid state UV-vis adsorption spectrum (a) and Tauc's plot for band gap (b) of [BuDA]Cu₂Br₄.

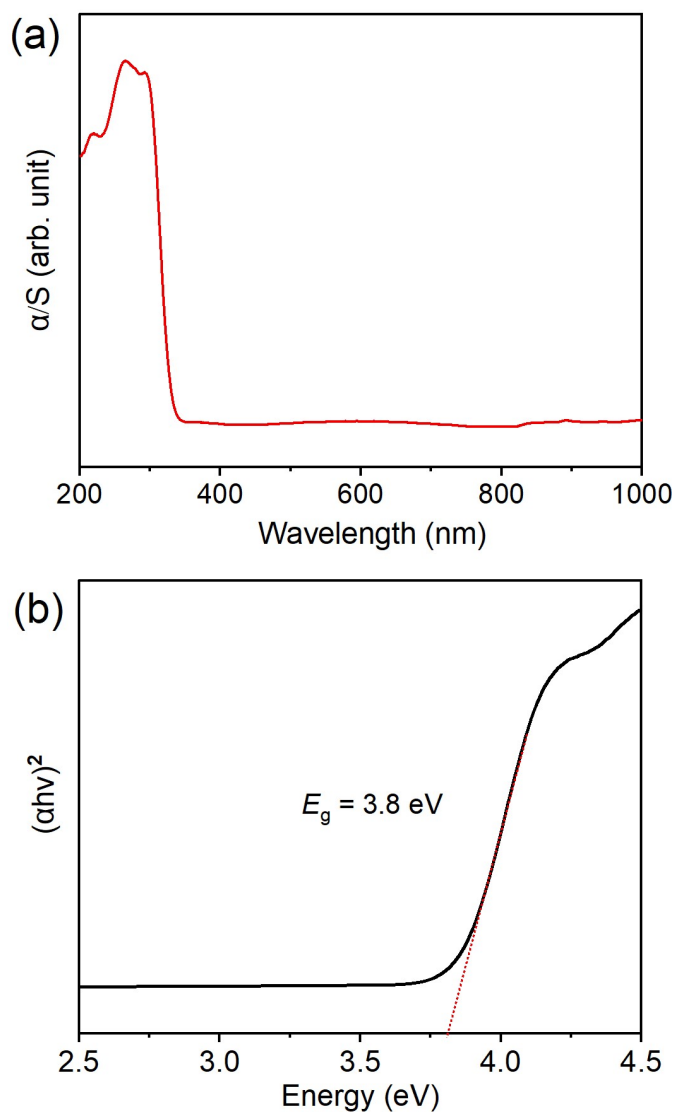


Fig. S4 The solid state UV-vis adsorption spectrum (a) and Tauc plot for band gap (b) of [TMEDA]Cu₂Br₄.

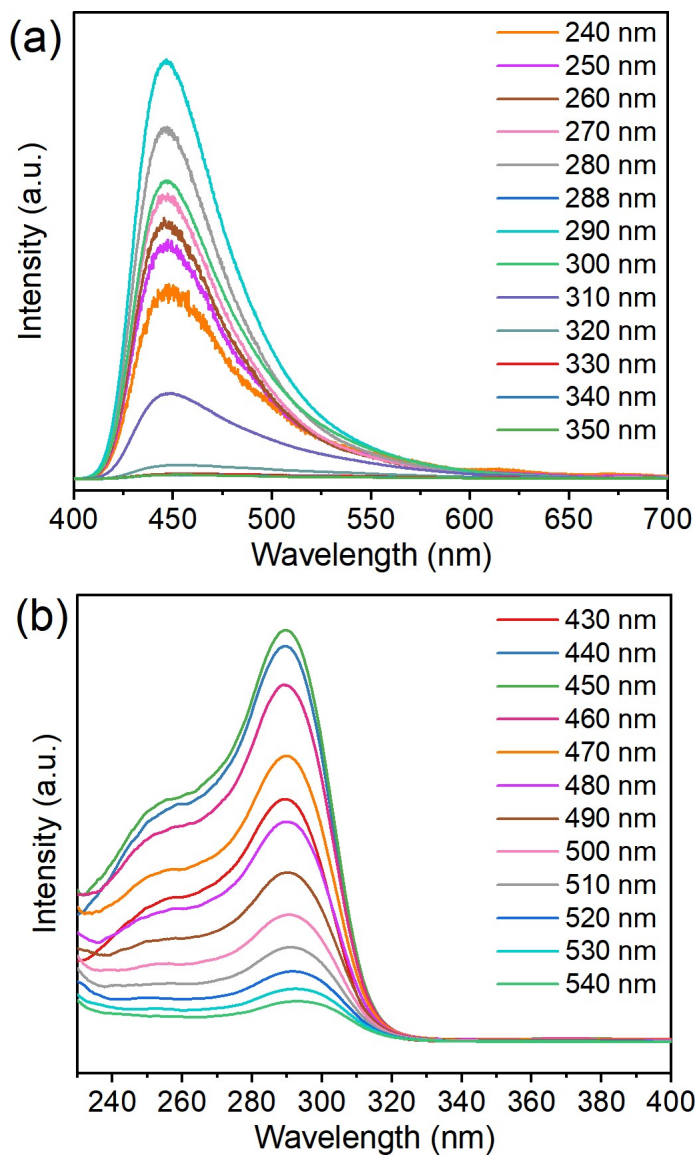


Fig. S5 (a) The excitation wavelength dependent PL emission spectra, and (b) the emission wavelength dependent PL excitation spectra of $[(\text{Me})_4\text{-Pipz}]\text{Cu}_2\text{Br}_4$.



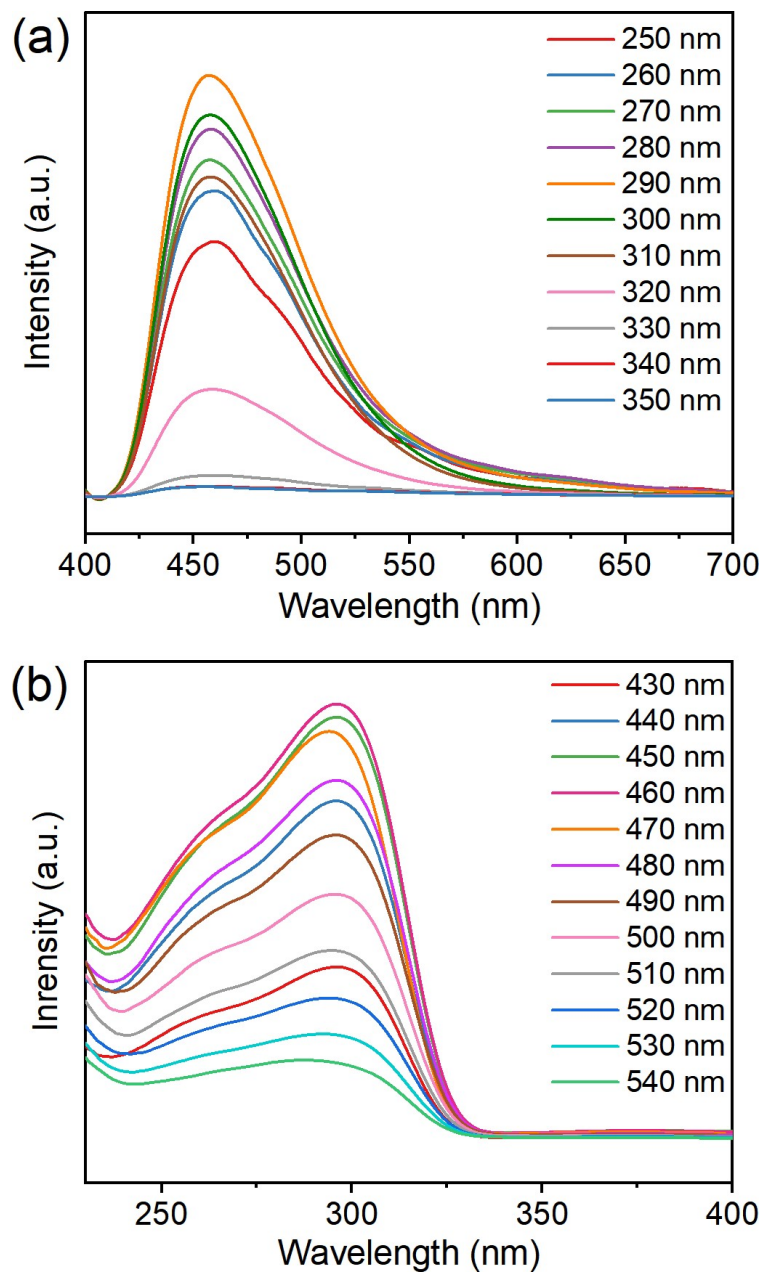


Fig. S6 (a) The excitation wavelength dependent PL spectra and (b) the emission wavelength dependent PL excitation spectra of $[BuDA]Cu_2Br_4$.

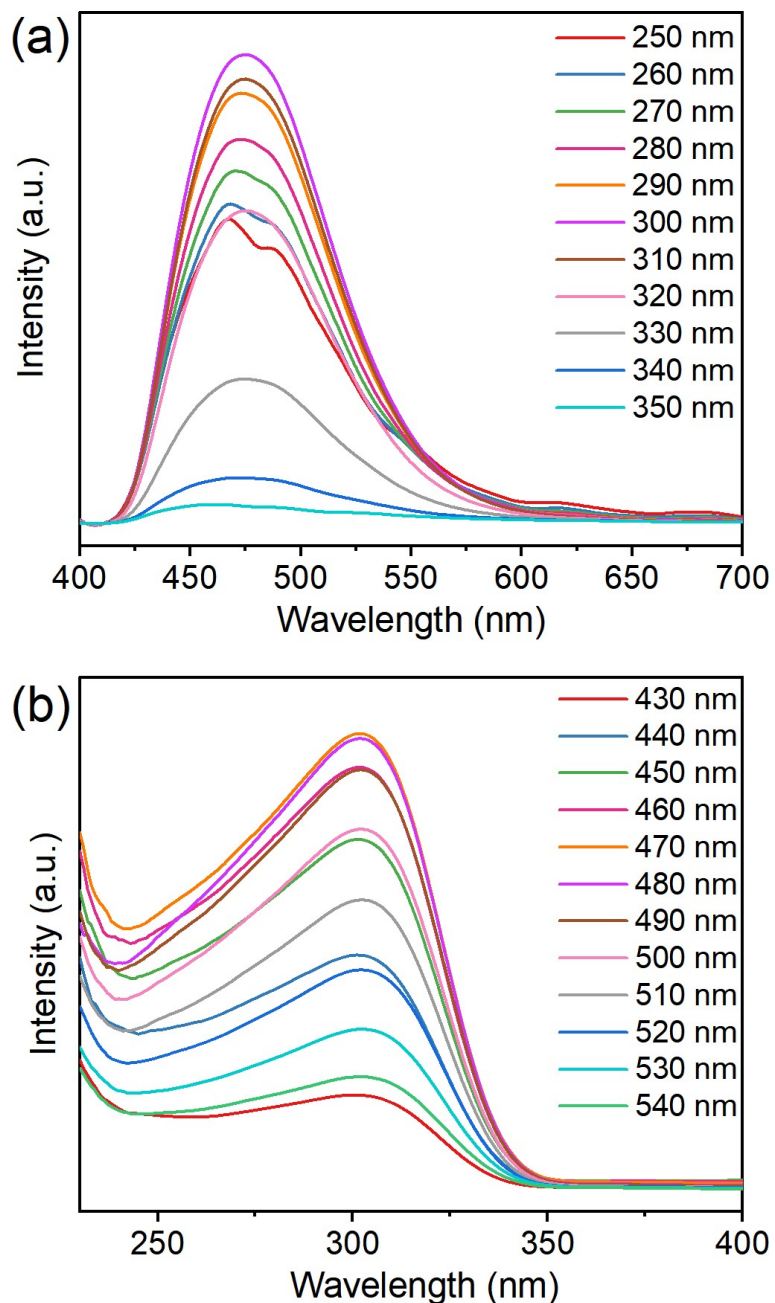


Fig. S7 (a) The excitation wavelength dependent PL spectra and (b) the emission wavelength dependent PL excitation spectra of [TMEDA]Cu₂Br₄.

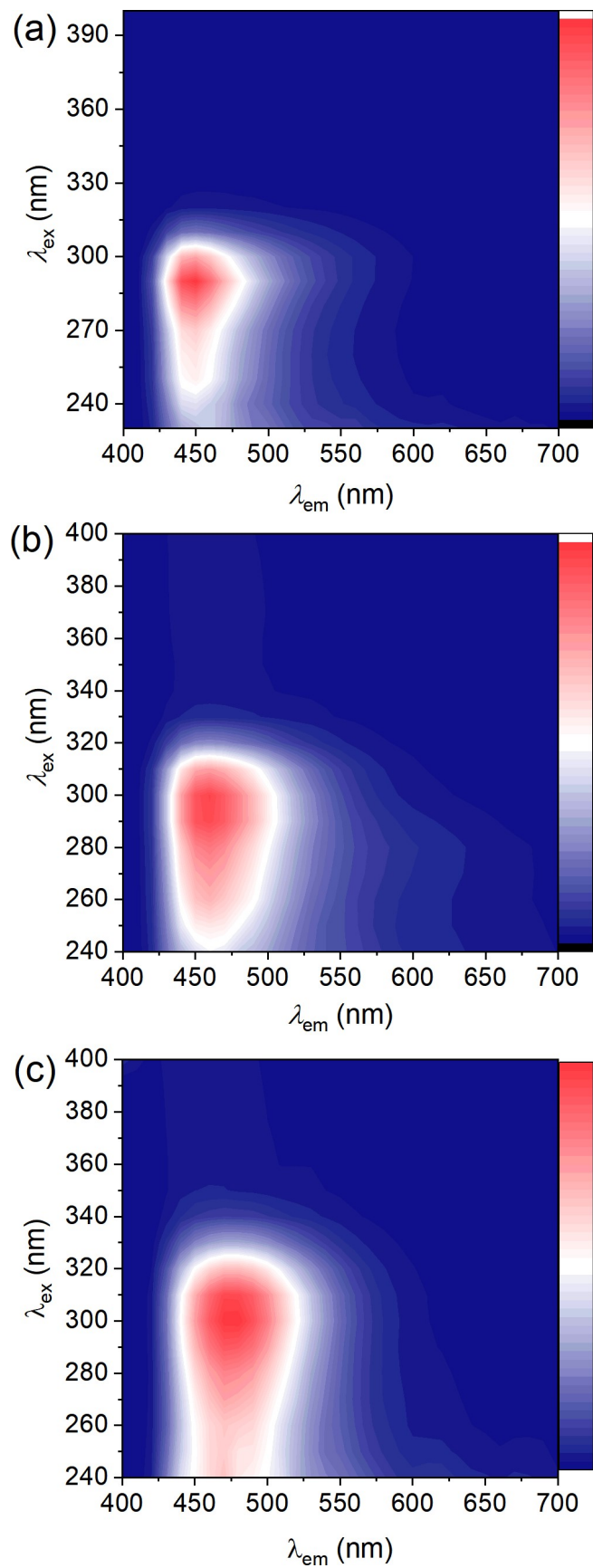


Fig. S8 3D consecutive PL excitation and emission correlation maps of (a) [(Me)₄-Pipz]Cu₂Br₄; (b) [BuDA]Cu₂Br₄ and (c) [TMEDA]Cu₂Br₄.

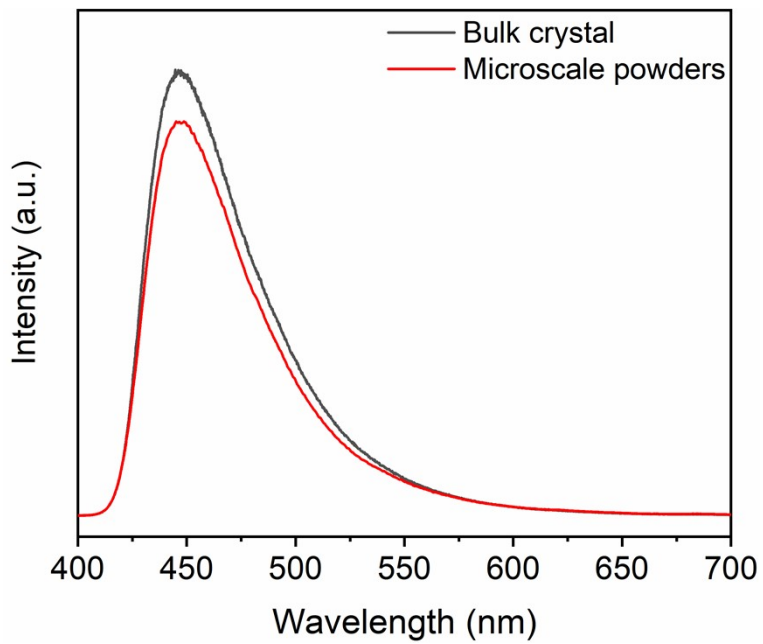


Fig. S9 Comparison of PL emission spectra of bulk crystals and microscale powders for $[(\text{Me})_4\text{-Pipz}]\text{Cu}_2\text{Br}_4$.

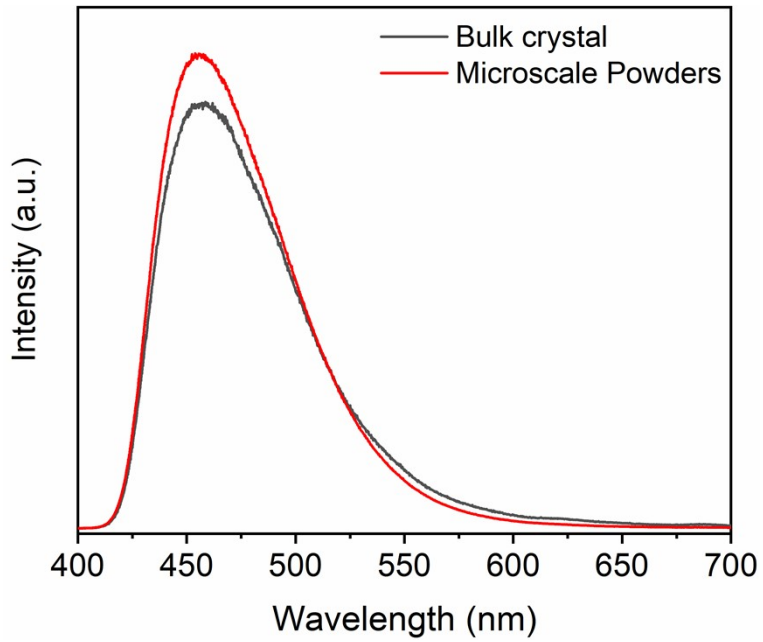


Fig. S10 Comparison of PL emission spectra of bulk crystals and microscale powders for $[\text{BuDA}]\text{Cu}_2\text{Br}_4$.

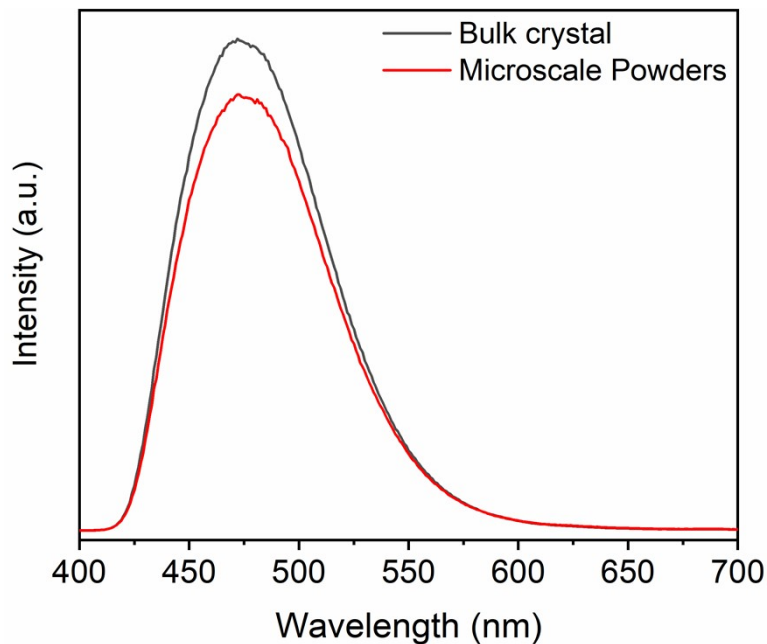


Fig. S11 Comparison of PL emission spectra of bulk crystals and microscale powders for $[(\text{TMEDA})_4\text{Cu}_2\text{Br}_4]$.

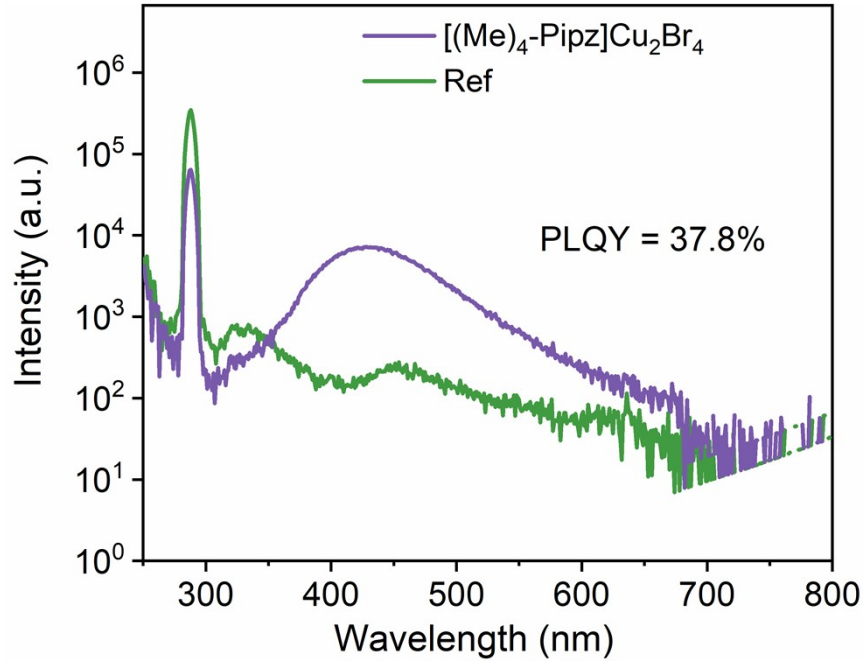


Fig. S12 The PLQY of $[(\text{Me})_4\text{-Pipz}]\text{Cu}_2\text{Br}_4$.

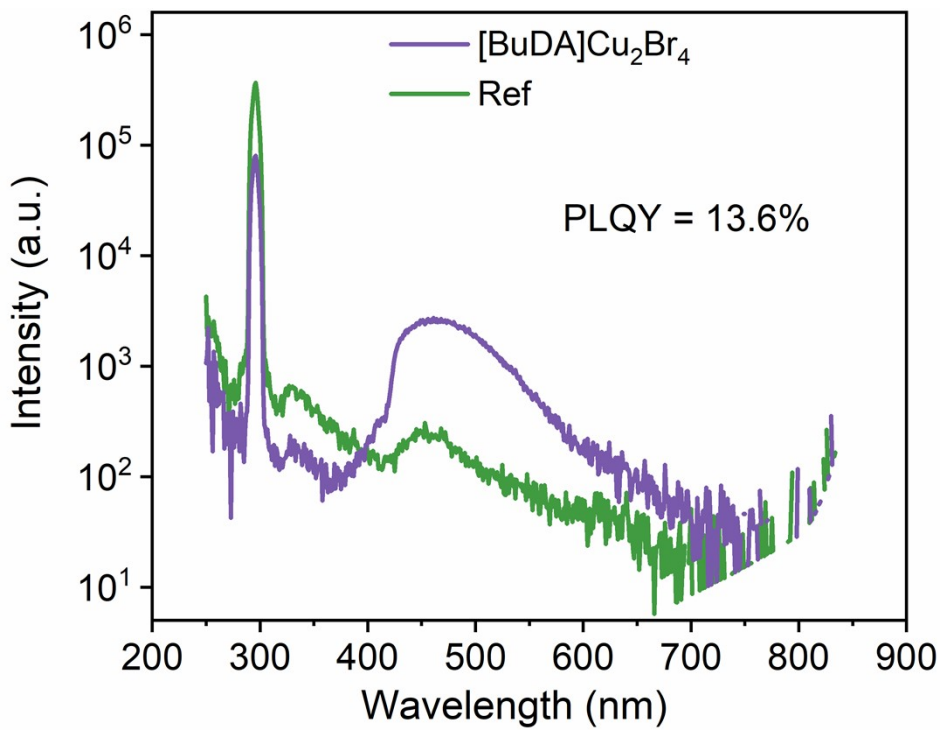


Fig. S13 The PLQY of $[\text{BuDA}]\text{Cu}_2\text{Br}_4$.

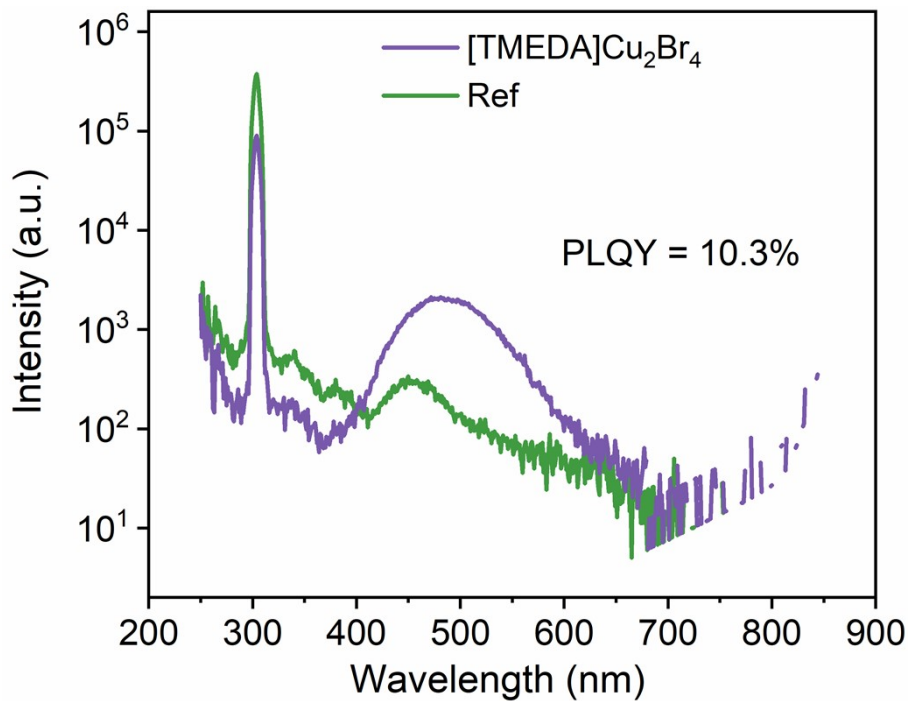


Fig. S14 The PLQY of $[\text{TMEDA}]\text{Cu}_2\text{Br}_4$.

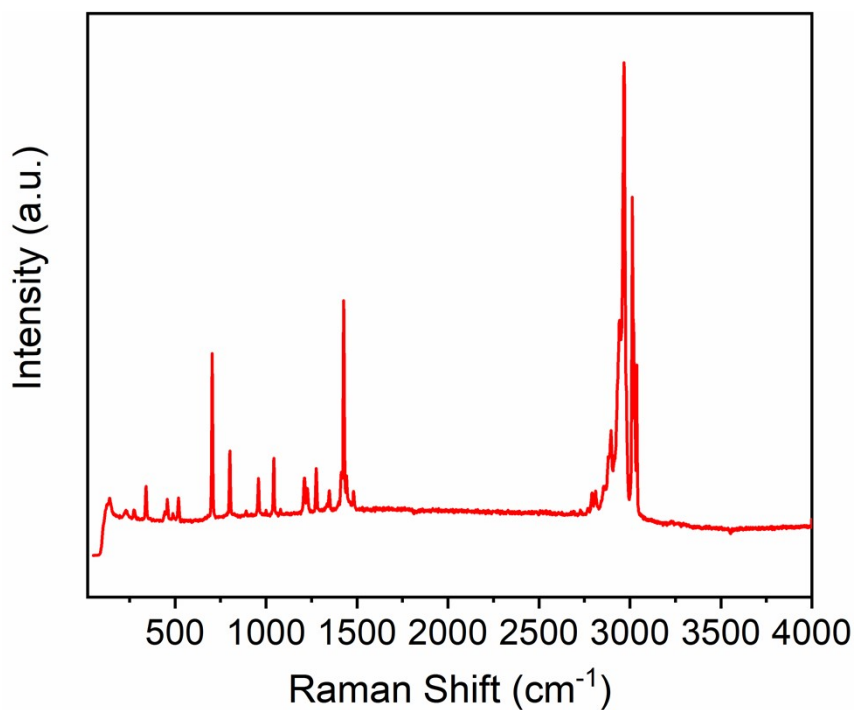


Fig. S15 Raman spectrum of $[(\text{Me})_4\text{-Pipz}] \text{Cu}_2\text{Br}_4$.

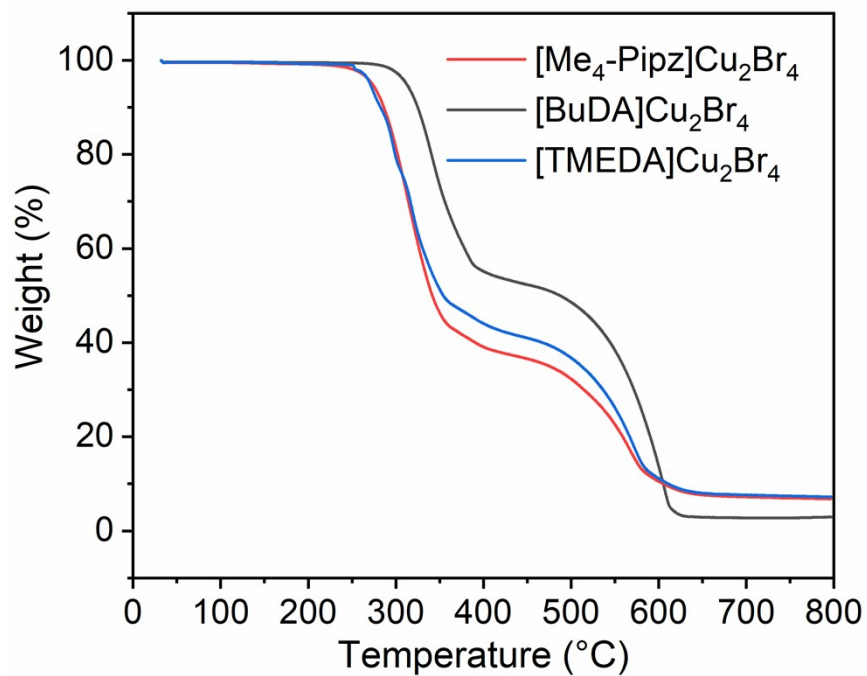


Fig. S16 The thermogravimetric analysis (TGA) curves of $[(\text{Me})_4\text{-Pipz}] \text{Cu}_2\text{Br}_4$, $[\text{BuDA}] \text{Cu}_2\text{Br}_4$ and $[\text{TMEDA}] \text{Cu}_2\text{Br}_4$.

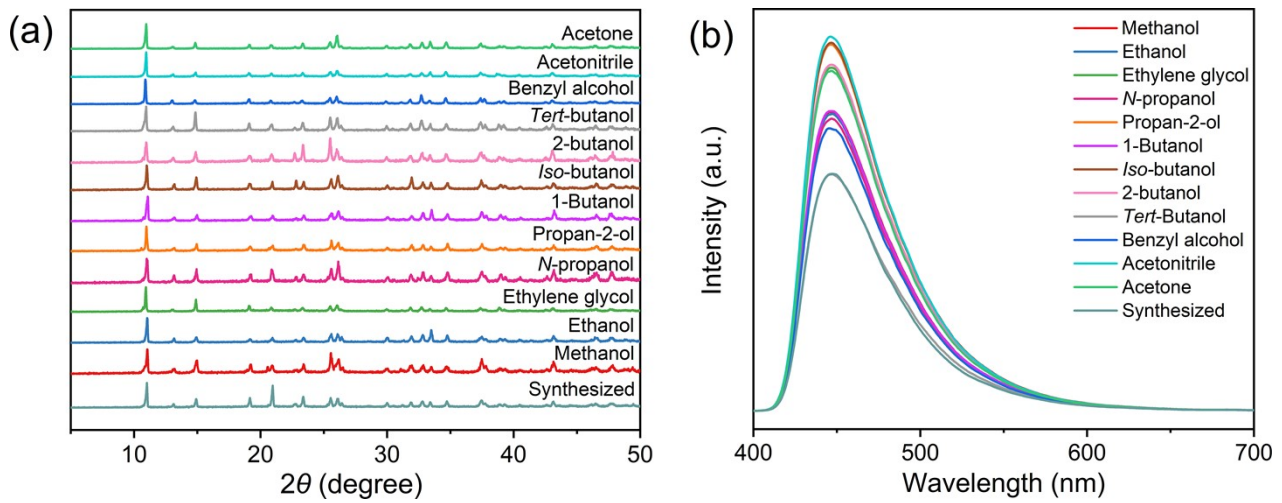


Fig. S17 PXRD patterns and PL emission spectra of $[(Me)_4\text{-Pipz}]Cu_2\text{Br}_4$ after immersing in various organic solvents.

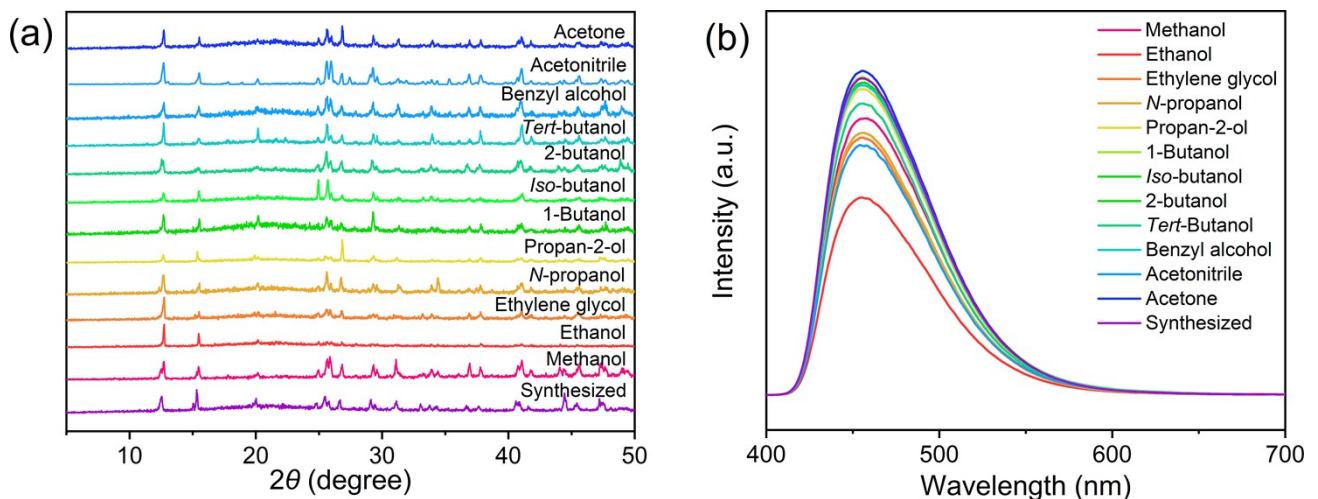


Fig. S18 PXRD patterns and PL emission spectra of $[\text{BuDA}]Cu_2\text{Br}_4$ after immersing in various organic solvents.

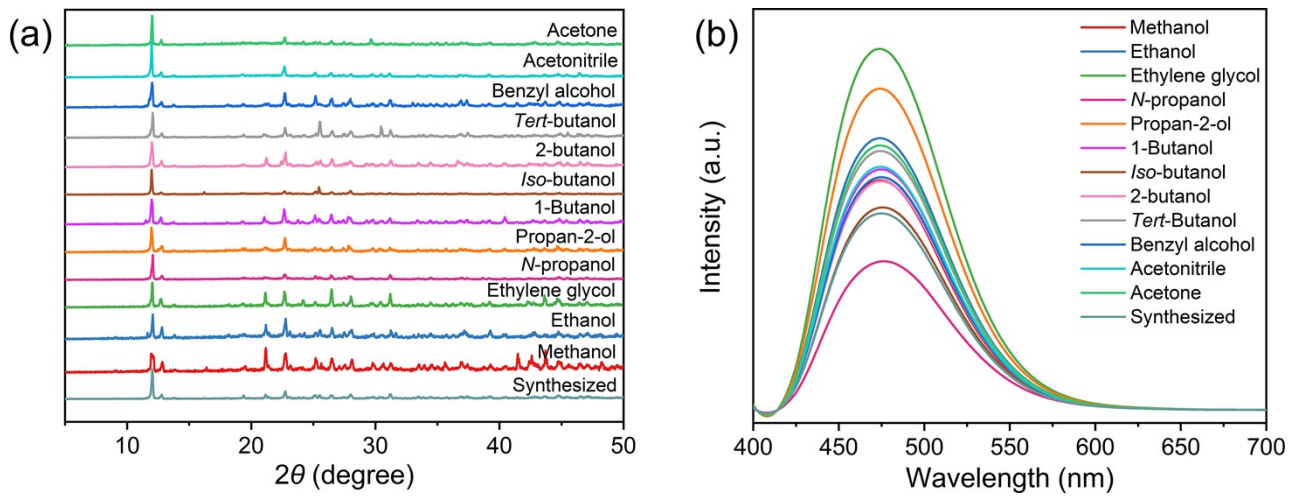


Fig. S19 PXRD patterns and PL emission spectra of $[\text{TMEDA}]\text{Cu}_2\text{Br}_4$ after immersing in various organic solvents.

Table S1. Crystal Data and Structural Refinements for [(Me)₄-Pipz]Cu₂Br₄.

Compound	[(Me) ₄ -Pipz]Cu ₂ Br ₄
Chemical formula	C ₈ N ₂ H ₂₀ Cu ₂ Br ₄
FW	295.49
Space group	<i>C</i> 2/ <i>m</i>
<i>a</i> /Å	13.848(4)
<i>b</i> /Å	6.7421(19)
<i>c</i> /Å	9.389(3)
$\alpha/^\circ$	90
$\beta/^\circ$	121.275(2)
$\gamma/^\circ$	90
<i>V</i> (Å ³)	749.2(4)
<i>Z</i>	4
<i>D</i> _{calcd} (g·cm ⁻³)	2.620
Temp (K)	296.15
μ (mm ⁻¹)	13.481
<i>F</i> (000)	560.0
Reflections collected	4263
Unique reflections	922
GOF on <i>F</i> ²	1.131
^a <i>R</i> ₁ , <i>wR</i> ₂ (<i>I</i> > 2σ(<i>I</i>))	0.0322/0.0834
^b <i>R</i> ₁ , <i>wR</i> ₂ (all data)	0.0361/0.0852

^a*R*₁ = $\sum ||F_o| - |F_c|| / \sum |F_o|$. ^b*wR*₂ = [$\sum w(F_o^2 - F_c^2)^2 / \sum w(F_o^2)^2$]^{1/2}.

Table S2. Crystal Data and Structural Refinements for [BuDA]Cu₂Br₄.

Compound	[BuDA]Cu ₂ Br ₄
Chemical formula	C ₄ N ₂ H ₁₄ Cu ₂ Br ₄
FW	268.45
Space group	P2 ₁ /n
a/Å	6.0905(3)
b/Å	8.8163(5)
c/Å	11.5467(6)
α/°	90
β/°	97.583(2)
γ/°	90
V(Å ³)	614.59(6)
Z	4
D _{calcd} (g·cm ⁻³)	2.901
Temp (K)	273.15
μ(mm ⁻¹)	16.419
F(000)	500.0
Reflections collected	6960
Unique reflections	1097
GOF on F ²	1.044
^a R ₁ ,wR ₂ (I > 2σ(I))	0.0236/0.0488
^b R ₁ ,wR ₂ (all data)	0.0330/0.0518

^aR_I = Σ||F_o| - |F_c||/Σ|F_o|. ^bwR₂ = [Σw(F_o² - F_c²)²/Σw(F_o²)²]^{1/2}.

Table S3. Crystal Data and Structural Refinements for [TMEDA]Cu₂Br₄.

Compound	[TMEDA]Cu ₂ Br ₄
Chemical formula	C ₆ N ₂ H ₁₈ Cu ₂ Br ₄
FW	564.94
Space group	P2 ₁ /c
a/Å	7.8140(7)
b/Å	14.6335(13)
c/Å	12.9812(11)
α/°	90
β/°	93.824(3)
γ/°	90
V(Å ³)	1481.0(2)
Z	4
D _{calcd} (g·cm ⁻³)	2.534
Temp (K)	273.15
μ(mm ⁻¹)	13.633
F(000)	1064.0
Reflections collected	16515
Unique reflections	2616
GOF on F ²	1.028
^a R ₁ ,wR ₂ (I > 2σ(I))	0.0345/0.0656
^b R ₁ ,wR ₂ (all data)	0.0682/0.0762

^aR_I = Σ||F_o| - |F_c||/Σ|F_o|. ^bwR₂ = [Σw(F_o² - F_c²)²/Σw(F_o²)²]^{1/2}.

Table S4. Hydrogen bonds data for $[(\text{Me})_4\text{-Pipz}]\text{Cu}_2\text{Br}_4$.

D-H \cdots A	d(D-H)	d(H \cdots A)	d(D \cdots A)	$\angle(\text{DHA})$
C1-H2 \cdots Br2 ¹	0.96	3.03	3.772(3)	135.5
C1-H3 \cdots Br2 ²	0.96	3.19	3.862(6)	128.3
C2-H4 \cdots Br1 ³	0.96	2.89	3.804(7)	159.2
C2-H5 \cdots Br1 ⁴	0.96	2.83	3.765(3)	164.9
C2-H6 \cdots Br1 ⁴	0.96	2.89	3.765(3)	152.8
C3-H7 \cdots Br2 ⁵	0.97	3.18	3.808(4)	124.1
C3-H8 \cdots Br2 ⁶	0.97	2.97	3.633(4)	126.5

¹1/2+x, 1/2+y, +z; ²1-x, +y, 1-z; ³3/2-x, 1/2+y, 2-z; ⁴+x, 1+y, +z; ⁵1/2+x, -1/2+y, +z; ⁶3/2-x, -1/2+y, 2-z